J Toxicol Pathol 2013; 26: 423–427

Case Report

Immunohistochemical Characterization of a Renal Nephroblastoma in a *Trp*53-mutant and Prolyl Isomerase 1-deficient Mouse

Vittoria Castiglioni[1,2*], Marcella De Maglie[2], Roberta Queliti[3], Alessandra Rustighi[4,5], Giannino Del Sal[4,5], and Enrico Radaelli[1,2]

[1] Dipartimento di Scienze Veterinarie e Sanità Pubblica Veterinaria (DIVET), Facolta di Medicina Veterinaria, Università degli Studi di Milano, Via Celoria, 10, 20133 Milano, Italy
[2] Mouse & Animal Pathology Lab, Fondazione Filarete, Viale Ortles, 22/4, 20139 Milano, Italy
[3] Centro Ricerche Bracco, Bracco Imaging Spa, via Ribes 5, 10010 Colleretto Giacosa (TO), Italy
[4] Laboratorio Nazionale CIB (LNCIB), Area Science Park, 34149 Trieste, Italy
[5] Dipartimento di Scienze della Vita, Università degli Studi di Trieste, 34127 Trieste, Italy

Abstract: A nephroblastoma is a tumor arising from metanephric blastema occurring in childhood. Among laboratory rodents, nephroblastoma has been frequently reported in rats, but it remains exceedingly rare in mice. The present work describes a nephroblastoma in a young mouse homozygous for the specific Trp53 R172H point mutation coupled with targeted deletion of the *Pin1* gene. The affected kidney was effaced by a biphasic tumor with an epithelial component arranged in tubules surrounded by nests of blastemal cells. Immunohistochemically, the neoplasm was diffusely positive for Wilms' tumor antigen. The epithelial component expressed markers of renal tubular differentiation including wide-spectrum cytokeratin, E-cadherin and folate-binding protein. Furthermore, the neoplasm exhibited a high proliferative index and diffuse nucleocytoplasmic β-catenin expression. Based on histological and immunohistochemical features, a diagnosis of nephroblastoma potentially associated with *Trp53* loss and oncogenic β-catenin activation has been proposed. (DOI: 10.1293/tox.2013-0021; J Toxicol Pathol 2013; 26: 423–427)

Key words: immunohistochemistry, kidney, mouse, nephroblastoma, pathogenesis

A nephroblastoma, also known as a "embryonal nephroma" and/or "Wilms' tumor", is an embryonal renal tumor originating from metanephric blastema, which is usually described as composed of a mixture of three cell populations: epithelial, mesenchymal and blastemal cells[1]. A nephroblastoma generally arises at one pole of the kidney, and it is considered a malignant neoplasm with metastatic potential[1].

Wilms' tumor is the most common primary renal tumor of childhood, with a peak incidence between 2 and 3 years of age[2]. The pathogenesis of nephroblastoma has been extensively investigated in human medicine, and genetic alterations have been associated with this malignancy. Mutations of three tumor-suppressor genes (Wilms' tumor 1, *WT1*; Wilms' tumor gene on the X chromosome, *WTX;* and *TP53*) and one oncogene (*CTNNB1*) are reported to occur either singly or in combination[3].

Considering nonhuman species, nephroblastoma is the most common primary renal tumor of pigs[4] and chickens[5]. Nephroblastomas occur far less often in calves[6] and dogs[7] and are occasionally reported in sheep[8], horses[9], cats[10] and fishes[11]. As in humans, nephroblastomas in these animal species are mainly described in young subjects, with only a minority of cases occurring in adults. With reference to laboratory animals, nephroblastomas are commonly described in rats, both as spontaneous[12] and experimentally-induced[13,14] lesions, and are extremely rare in nonhuman primates[15,16] and mice[17–19], with only few cases reported so far.

The aim of this study was to describe the pathological and immunohistochemical features of a renal nephroblastoma spontaneously occurring in a genetically engineered young mouse and provide some insights into tumor pathogenesis.

The animal considered in this study was a 15-week-old male mouse belonging to a genetically engineered line characterized by Trp53 R172H point mutation on both the alleles coupled with targeted deletion of the *Pin1* gene[20]. Mice from this cohort were maintained on a C57BL/6 background. The mouse was sacrificed because of generalized deterioration of clinical conditions and marked abdominal enlargement. A complete necropsy was performed, and samples of representative organs were obtained for histological examination. Samples were trimmed, fixed in 10% buffered formalin, paraffin-embedded, sectioned at four μm and stained with

Received: 25 April 2013, Accepted: 8 July 2013
*Corresponding author: V Castiglioni (e-mail: vittoria.castiglioni@unimi.it)

Table 1. Details Concerning Primary Antibodies and Procedures Used for the Immunohistochemical Examination of the Renal Nephroblastoma Reported in This Study

Antigen	Primary antibody	Source	Antigen retrieval	Working dilution	Incubation time	Detection system
β-catenin	6B3 Rb mon[a]	Cell signaling	HIER[c]	1:150	1,5 h RT[e]	ABC[f]
Wide-spectrum cytokeratin (WSCK)	Z0622 Rb poly[b]	Dako	Enzymatic digestion[d]	1:600	1h RT[e]	ABC[f]
E-cadherin	EP913(2)Y Rb mon[a]	Epitomics	HIER[c]	1:600	1h RT[e]	ABC[f]
Folate-binding protein (FBP)	ab67422 Rb poly[b]	Abcam	HIER[c]	1:1200	1h RT[e]	ABC[f]
Ki67	#RM-9106-S Rb mon[a]	LabVision (Thermo Scientific)	HIER[c]	1:200	1h RT[e]	EnVision[g]
Smooth muscle actin (SMA)	#1184-1 Rb mon[a]	Epitomics	HIER[c]	1:150	1h RT[e]	EnVision[g]
Vimentin	EPR3776 Rb mon[a]	Epitomics	HIER[c]	1:500	1h RT[e]	ABC[f]
Wilms' tumor antigen 1 (WT1)	CAN-R9(IHC)-56-2 Rb mon[a]	Epitomics	HIER[c]	1:100	1h RT[e]	ABC[f]

[a] Rabbit monoclonal; [b] Rabbit polyclonal; [c] heat-induced epitope retrieval, citrate buffer pH=6.0; [d] Digest-all™3 Pepsin solution RTU (Invitrogen Corporation, Camarillo, CA, USA); [e] one hour at room temperature; [f] Avidin-biotin complex (Vectastain Elite ABC kit PK-6100, Vector Laboratories Inc., Burlingame, CA, USA); [g] Dako EnVision™ System (DakoCytomation, Glostrup, Denmark).

hematoxylin and eosin for histopathological examination. Immunohistochemical analysis was performed in order to confirm the diagnostic hypothesis and to get some insights into the possible pathogenesis of the lesion. Details concerning the panel of immunohistochemical stains applied are listed in Table 1. Negative immunohistochemical controls were prepared by replacing the primary antibody with an irrelevant one, and known positive control sections were included in each immunolabeling assay.

Procedures involving animals and their care conformed to institutional guidelines in compliance with national (D.L.vo 116/92 and following additions) and international (EEC Council Directive 86/609, OJ L 358, 1, 12-12-1987; NIH Guide for the Care and Use of Laboratory Animals, U.S. National Research Council, 1996) laws and policies.

At necropsy, ascites was detected, and the left kidney was markedly enlarged by a multinodular, tan and hemorrhagic mass that was up to 1.5 × 3 cm in diameter.

Histologically, the renal parenchyma was completely effaced by a densely cellular, partially encapsulated, lobulated mass composed of a mixture of 2 main cell populations and supported by a minimal amount of stroma. The first population consisted of neoplastic epithelial cells arranged in single-layered infolded tubules, which were occasionally filled by necrotic debris (Fig. 1A). Cells were 12–15 μm in diameter and cuboidal to columnar, with distinct cell borders, an intermediate nuclear to cytoplasmic ratio and a moderate amount of pale eosinophilic homogeneous cytoplasm. Nuclei were oval, 10 μm in diameter and central to paracentral with coarsely clumped chromatin and occasionally had an evident nucleolus. Anisocytosis and anisokaryosis were mild; mitoses were rare. The second population of cells (neoplastic blastemal cells) was arranged in closely packed nests centered around the aforementioned tubules (Fig. 1A). Cells were polygonal and up to 20 μm in diameter, with variably distinct cell borders, a high nuclear to cytoplasmic ratio and a scant amount of pale eosinophilic homogeneous cytoplasm. Nuclei were central, 15 μm in diameter and oval with densely clumped chromatin and no evident nucleoli. Anisocytosis and anisokaryosis were moderate to marked, there were 3–6 mitoses per high-power field, often with a bizarre morphology and there were large numbers of scattered apoptotic cells. Closely intermingled with these two atypical cell populations were lesser numbers of atypical spindle cells (neoplastic mesenchymal cells) with indistinct cell borders, an intermediate nuclear to cytoplasmic ratio and a moderate amount of pale eosinophilic homogeneous cytoplasm. Nuclei were central, oval, plump and approximately 15–20 μm in diameter, with marginated chromatin and 1–2 nucleoli. Anisocytosis and anisokaryosis were moderate, and mitoses were rare. Centrally the tumor was effaced by wide coalescing areas of coagulative necrosis and hemorrhages. The perirenal adipose tissue was expanded by moderate numbers of lymphocytes, plasma cells and macrophages, occasionally with their cytoplasm filled by erythrocytes (erythrophagocytosis). Morphologically, the tumor was consistent with a diagnosis of renal nephroblastoma.

The immunohistochemical profile of the different neoplastic cell populations is summarized in Table 2. Briefly, neoplastic cells belonging to both the epithelial and blastemal components were diffusely positive for Wilms' tumor antigen 1 and negative for vimentin (Figs. 1B and 1C). The epithelial population arranged in tubules was diffusely positive for wide-spectrum cytokeratin (WSCK) (Fig. 1D), E-cadherin and to a lesser degree for folate-binding Protein (FBP) (Fig. 1E). Smooth muscle actin (SMA) immunohistochemistry highlighted the presence of few scattered intratumoral clusters of atypical spindle cells (Fig. 1F), which were also variably positive for Wilms' tumor antigen 1. Furthermore, there was diffuse nuclear positivity for Ki-67 within the blastemal cellular population, whereas lesser numbers of positive nuclei were detected within the epithelial cellular population (Fig. 1G). A strong and diffuse nuclear and cytoplasmic positivity for β-catenin could be appreciated within epithelial and blastemal components (Fig. 1H).

Neither concomitant occurrence of other malignancies nor evidence of metastatic spreading were observed. Of interest, the relatively young age of the affected animal indicates that in mice, nephroblastoma may develop congeni-

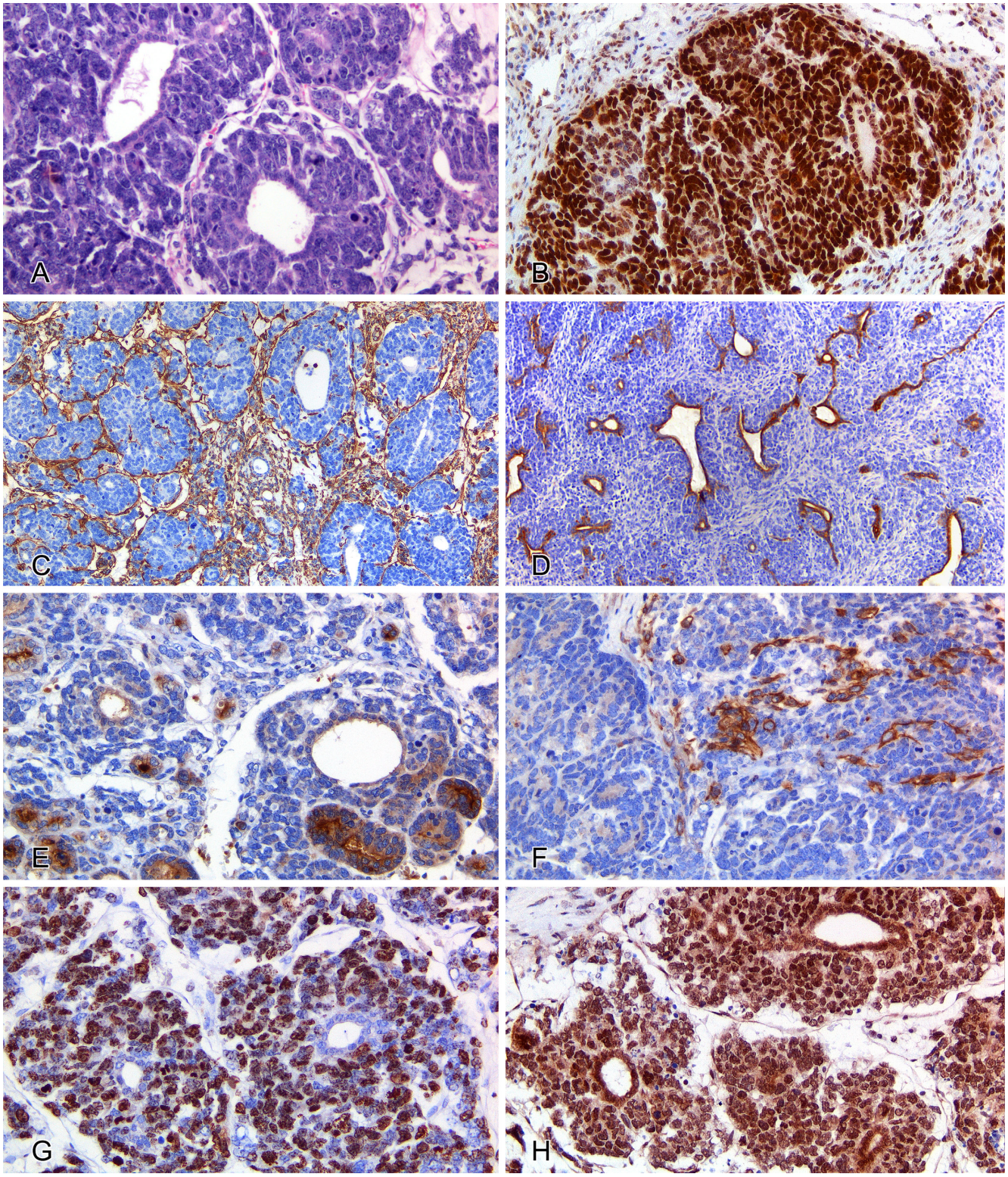

Fig. 1. Kidney; biphasic nephroblastoma in a *Trp53*-mutant and prolyl isomerase 1-deficient mouse. (A) The tumor is composed of neoplastic epithelial cells arranged in single-layered tubules surrounded by neoplastic blastemal cells arranged in nests. Hematoxylin and eosin, 200×. (B) Both epithelial and blastemal cell populations are characterized by marked and diffuse nuclear immunoreactivity for Wilms' tumor antigen 1. Wilms' tumor antigen 1 immunohistochemistry (IHC), 200×. (C) Scant cytoplasmic immunoreactivity for vimentin is observed in the stromal compartment separating neoplastic cell populations. Vimentin IHC, 100×. (D) Neoplastic epithelial cells lining tubules diffusely express cytokeratin. Wide spectrum cytokeratin IHC, 100×. (E) Scattered tubules display FBP immunoreactivity, which is mainly concentrated along the luminal surface of neoplastic epithelial cells. FBP IHC, 200×. (F) Few scattered neoplastic mesenchymal cells are diffusely positive for smooth muscle actin (SMA). SMA IHC, 200×. (G) A large number of Ki-67-positive neoplastic cells are evident in the blastemal compartment, whereas only scattered Ki-67-positive neoplastic epithelial cells line the tubular structures. Ki-67 IHC, 200×. (H) Both epithelial and blastemal cell populations are characterized by marked and diffuse nuclear and cytoplasmic immunoreactivity for β-catenin. β-catenin IHC, 200×.

Table 2. Summary of the Immunohistochemical Phenotype Displayed by Epithelial, Blastemal and Mesenchymal Components in Examined Renal Murine Neoplasm

Stain	Epithelial	Blastemal	Mesenchymal
WT1	+++ n	+++ n	+ n
Vimentin	-	-	+++ c
WSCK	+++ mc	-	-
E-cadherin	+++ mc	-	-
FBP	+ mc	-	-
SMA	-	-	++ c
Ki-67	+ n	+++ n	-
β-catenin	+++ nc	+++ nc	-

(-) no detectable immunoreactivity/stain; (+) immunoreactivity/stain accounting for less than 10% of the considered cell population; (++) immunoreactivity/stain comprised between 20% and 60% of the considered cell population; (+++) immunoreactivity/ stain accounting for more than 60% of the considered cell population; c= cytoplasmic immunoreactivity; mc= membranous to cytoplasmic immunoreactivity; n= nuclear immunoreactivity; nc= nuclear to cytoplasmic immunoreactivity.

tally or as a neonatal lesion, as in other species.

The nephroblastoma examined here was mainly composed of two cell populations (namely, epithelial and blastemal cells) with an inconspicuous mesenchymal component. In this context, the tumor was further subclassified as a "biphasic nephroblastoma." Notably, the neoplastic epithelial component detected in the examined case was composed of cells arranged in tubules with no evidence of primitive glomeruli formation. Though the formation of tufts of atypical epithelial cells projecting into lumina (primitive glomeruli) is a feature commonly associated with these neoplasms, the presence of these structures is not essential for a diagnosis of nephroblastoma. The evidence of a highly basophilic blastema combined with structures differentiating into nephric elements (tubules in this case) are instead mandatory requirements to classify a lesion in the aforementioned category[21]. Furthermore, a classification into different nephroblastoma subtypes based on their histological characteristics and on their relative contents of epithelial and mesenchymal elements has already been performed in swine with the nephroblastic, epithelial, mesenchymal and miscellaneous subtypes described[4]. No metastatic spreading of the disease was observed in this case. Although metastatic dissemination to multiple organs has been described in renal nephroblastomas affecting rats[12], no data regarding metastatic dissemination of murine nephroblastomas have been reported so far.

The diffuse positivity observed for Wilms' tumor antigen 1 confirmed the diagnostic hypothesis of renal nephroblastoma, and this marker was combined with a broader immunohistochemical panel with the aim of better characterizing the renal neoplasm. Tubular positivity for WSCK, E-cadherin and FBP could be interpreted as an attempt of the tumor to differentiate into tubules, considering that FBP is specifically expressed by renal proximal tubules[22] and E-cadherin has a robust expression in the ureteric bud-derived components of the kidney[23]. The paucity of SMA-positive atypical spindle cells supported the notion of a "biphasic" nephroblastoma with minimal mesenchymal differentiation towards smooth muscle tissue.

Further immunohistochemical markers were performed in order to better clarify the molecular scenario in which the malignancy arose and to speculate regarding tumor pathobiology. With respect to tumor proliferative index, the three histological components of nephroblastomas (blastemal, epithelial and stromal) are known to have different proliferative potentials, with the highest proliferative index reported to occur in the epithelium[24–27]. The rationale behind this finding has not been fully elucidated so far, since the epithelial component is universally considered to be more differentiated than the other ones[26,27]. In contrast, in the case reported here, the greatest number of Ki-67 positive nuclei was observed in the blastemal population, a finding that mirrors the assumption that the blastema is less mature and less differentiated than the other components[26,27]. Furthermore, the Ki-67 proliferation index in blastemal cells is reported to be an indicator of metastatic potential[28], but no evidence of metastatic spreading was observed in the examined case, despite the exceedingly high numbers of blastemal Ki-67-positive nuclei observed.

Mutations occurring in human nephroblastomas involve three tumor-suppressor genes (Wilms' tumor 1, *WT1*; Wilms' tumor gene on the X chromosome; *WTX;* and *TP53*) and one oncogene (*CTNNB1*). In the present case, the diffuse expression of β-catenin observed in both the nucleus and the cytoplasm of neoplastic cells is highly suggestive of an activation of the Wnt oncogenic pathway. β-catenin is encoded by the *CTNNB1* gene and is known to undergo somatic stabilizing mutations in human nephroblastomas[3,23], and it has already been described to be overexpressed in rat nephroblastomas[29]. In the examined case, Trp53 function was also compromised by the specific R172H point mutation. Taken together, these two latter aspects suggest that in this mouse, the combined effect of *Trp53* loss and oncogenic β-catenin activation may have played a primary role in nephroblastoma development. It would be extremely intriguing to further investigate the status of WTX and WT1, known to be altered in human nephroblastoma, in order to clarify tumor pathogenesis in mice and compare it with the human counterpart.

In conclusion, to the authors' knowledge, this is the first report providing a detailed immunohistochemical description of nephroblastoma as an exceedingly rare spontaneous murine renal tumor potentially associated with *Trp53* loss and oncogenic β-catenin activation.

Acknowledgments: This work was supported by an AIRC Special Program Molecular Clinical Oncology ''5 per mille'' grant, grants from the Italian University and Research Ministerium (PRIN and FIRB grants), and a grant from Friuli-Venezia-Giulia (regional grant AITT) to G.D.S.

References

1. Grant Maxie M, and Newman SJ. Urinary system. In: Jubb, Kennedy, and Palmer's Pathology of Domestic Animals, 5th ed. Saunders Elsevier, Philadelphia. 501–503. 2007.
2. Pietras W. Advances and changes in the treatment of children with nephroblastoma. Adv Clin Exp Med. **21**: 809–820. 2012. [Medline]
3. Huff V. Wilms tumor genetics. Am J Med Genet. **79**: 260–267. 1998. [Medline]
4. Hayashi M, Tsuda H, Okumura M, Hirose M, and Ito N. Histopathological classification of nephroblastomas in slaughtered swine. J Comp Pathol. **96**: 35–46. 1986. [Medline]
5. Campbell JG, and Appleby EC. Tumours in young chickens bred for rapid body growth (broiler chickens): a study of 351 cases. J Pathol Bacteriol. **92**: 77–90. 1966. [Medline]
6. Yamamoto Y, Yamada M, Nakamura K, Takahashi Y, and Miyamoto T. Nephroblastoma with transcoelomic metastasis in a Japanese black bull. J Vet Med Sci. **68**: 891–893. 2006. [Medline]
7. Simpson RM, Gliatto JM, Casey HW, and Henk WG. The histologic, ultrastructural, and immunohistochemical features of a blastema-predominant canine nephroblastoma. Vet Pathol. **29**: 250–253. 1992. [Medline]
8. Headley SA, Saut JP, and Maiorka PC. Nephroblastoma in an adult sheep. Vet Rec. **159**: 850–852. 2006. [Medline]
9. Jardine JE, and Nesbit JW. Triphasic nephroblastoma in a horse. J Comp Pathol. **114**: 193–198. 1996. [Medline]
10. Henry CJ, Turnquist SE, Smith A, Graham JC, Thamm DH, O'Brien M, and Clifford CA. Primary renal tumours in cats: 19 cases (1992–1998). J Feline Med Surg. **1**: 165–170. 1999. [Medline]
11. Masahito P, Ishikawa T, Okamoto N, and Sugano H. Nephroblastomas in the Japanese eel, Anguilla japonica Temminck and Schlegel. Cancer Res. **52**: 2575–2579. 1992. [Medline]
12. Chandra M, and Carlton WW. Incidence, histopathologic and electron microscopic features of spontaneous nephroblastomas in rats. Toxicol Lett. **62**: 179–190. 1992. [Medline]
13. Li K, Gao J, Xiao X, Chen L, and Zhang L. The enhancing role of vitamin A deficiency on chemically induced nephroblastoma in rats. J Pediatr Surg. **40**: 1951–1956. 2005. [Medline]
14. Nagashima Y, Miyagi Y, Sumino K, Ohaki Y, Umeda M, Oshimura M, and Misugi K. Characterization of experimental rat nephroblastoma and its cell line. Tohoku J Exp Med. **168**: 303–305. 1992. [Medline]
15. Goens SD, Moore CM, Brasky KM, Frost PA, Leland MM, and Hubbard GB. Nephroblastomatosis and nephroblastoma in nonhuman primates. J Med Primatol. **34**: 165–170. 2005. [Medline]
16. Zöller M, Matz-Rensing K, Fahrion A, and Kaup FJ. Malignant nephroblastoma in a common marmoset (Callithrix jacchus). Vet Pathol. **45**: 80–84. 2008. [Medline]
17. Jackson Laboratory 1998. from Mouse tumor biology database: http://tumor.informatics.jax.org/mtbwi/index.do.
18. Liebelt AG, Sass B, Sobel HJ, and Werner RM. Spontaneous nephroblastoma in a strain CE/J mouse. A case report. Toxicol Pathol. **17**: 57–61. 1989. [Medline]
19. Shen KC, Heng H, Wang Y, Lu S, Liu G, Deng CX, Brooks SC, and Wang YA. ATM and p21 cooperate to suppress aneuploidy and subsequent tumor development. Cancer Res. **65**: 8747–8753. 2005. [Medline]
20. Girardini JE, Napoli M, Piazza S, Rustighi A, Marotta C, Radaelli E, Capaci V, Jordan L, Quinlan P, Thompson A, Mano M, Rosato A, Crook T, Scanziani E, Means AR, Lozano G, Schneider C, and Del Sal GA. Pin1/Mutant p53 axis promotes aggressiveness in breast cancer. Cancer Cell. **20**: 79–91. 2011. [Medline]
21. Frazier KS, Seely JC, Hard GC, Betton G, Burnett R, Nakatsuji S, Nishikawa A, Durchfeld-Meyer B, and Bube A. Proliferative and nonproliferative lesions of the rat and mouse urinary system. Toxicol Pathol. **40**: 14S–86S. 2012. [Medline]
22. Birn H, Selhub J, and Christensen EI. Internalization and intracellular transport of folate-binding protein in rat kidney proximal tubule. Am J Physiol. **264**: C302–C310. 1993. [Medline]
23. Hu Q, Gao F, Tian W, Cristy Ruteshouser E, Wang Y, Lazar A, Stewart J, Strong LC, Behringer RR, and Huff V. *Wt1* ablation and *Igf2* upregulation in mice result in Wilms tumors with elevated ERK1/2 phosphorylation. J Clin Invest. **121**: 174–183. 2011. [Medline]
24. Delahunt B, Farrant GJ, Bethwaite PB, Nacey JN, and Lewis ME. Assessment of proliferative activity in Wilms' tumor. Anal Cell Pathol. **7**: 127–138. 1994. [Medline]
25. Ghanem MA, Van der Kwast TH, Sudaryo MK, Mathoera RB, van der Heuvel MM, Al-Doray AA, Nijman RM, and van Steenbrugge GJ. MIB-1 (KI-67) proliferation index and cyclin-dependent kinase inhibitor p27Kip1 protein expression in nephroblastoma. Clinical Cancer Res. **10**: 591–597. 2004.
26. Jurić I, Pogorelić Z, Kuzmić-Prusac I, Biočić M, Jakovljević G, Stepan J, Župančić B, Čulić S, and Krušlin B. Expression and prognostic value of the Ki-67 in Wilms' tumor: experience with 48 cases. Pediatr Surg Int. **26**: 487–493. 2010. [Medline]
27. Khine MM, Aung W, Sibbons PD, Howard CV, Clapman E, McGill F, and Van Velzen D. Analysis of relative proliferation rates of Wilms' tumor components using proliferating cell nuclear antigen and MIB-1 (Ki-67 equivalent antigen) immunostaining and assessment of mitotic index. Lab Invest. **70**: 125–129. 1994. [Medline]
28. Berrebi D, Leclerc J, Schleiermacher G, Zaccaria I, Boccon-Gibod L, Fabre M, Jaubert F, El Ghoneimi A, Jeanpierre C, and Peuchmaur M. High cyclin E staining index in blastemal, stromal or epitehlial cells is correlated with tumor aggressiveness in patients with nephroblastoma. PLoS ONE. **3**: e2216. 2008. [Medline]
29. Ehrlich D, Bruder E, Thome MA, Gutt CN, von Knebel Doeberitz M, Niggli F, Perantoni AO, and Koesters R. Nuclear accumulation of β-catenin protein in chemically induced rat nephroblastomas. Pediatr Dev Pathol. **13**: 1–8. 2010. [Medline]